Title
Seismic Behaviors of Reinforced Concrete Column with Different Axial Compression Ratio Strengthened by Bidirectional Basalt Fiber-Reinforced Polymer (BFRP) Laminates

ISBN
978-3-031-76556-8

Authors
Peng, Gao
Zhonghui, Chen
Mosallam, Ayman S

Publication Date
2024

DOI
10.1007/978-3-031-76557-5_16

Seismic Behaviors of Reinforced Concrete Column with Different Axial Compression Ratio Strengthened by Bidirectional Basalt Fiber-Reinforced Polymer (BFRP) Laminates

Gao Peng[1], Chen Zhonghui[1], and Ayman S. Mosallam[2](✉)

[1] School of Civil Engineering, Hefei University of Technology, Hefei 230009, China
penggao@hfut.edu.cn, 2021110561@mail.hfut.edu.cn

[2] Department of Civil and Environmental Engineering, University of California, Irvine, USA
mosallam@uci.edu

Abstract. When existing reinforced concrete (RC) frame structures need seismic retrofitting, composite strengthening abilities including flexural, shear, and compressive load-bearing capacities are often required to be enhanced. The experimental research was conducted to investigate the seismic performance of RC columns confined with bidirectional fibers reinforced polymer (FRP) composite laminates. Three parameters were considered in this study: bidirectional fiber laminates, axial load ratio, and FRP anchors. Eight large-scale column specimens were evaluated experimentally and were subjected to low-frequency full-reversal cyclic lateral loadings up to failure. Experimental results indicated that the typical failure mode of columns confined with bidirectional fiber laminates differed significantly from that of unidirectional fiber laminates. Specimens strengthened with bidirectional fiber laminates exhibited a transition from bending-shear failure to bending failure, which resulted in fuller hysteresis loops, improved pinching behavior, and significantly enhanced energy dissipation and deformation capacity. After the specimen was confined, as the axial compression ratio increased within a certain range, the increase rate of bearing capacity decreased, and the increase of yield bearing capacity was more obvious than that of peak bearing capacity. The increase of axial compression ratio had little effect on the increase rate of displacement ductility, while the energy dissipation capacity increased obviously. The use of FRP anchors can further improve the bearing capacity and energy dissipation capacity of the specimen.

Keywords: Bidirectional fiber laminates · fiber anchor · axial compression ratio · seismic performance

1 Introduction

In seismic structural design, column fracture plays a crucial role in causing structural damage and collapse [1, 2]. Seismic performance of reinforced concrete (RC) structures depends on the deformability of columns [3, 4]. For the last decades, Fiber Reinforced

A. S. Mosallam et al. (Eds.): ICATH 2023, SCI, pp. 201–212, 2024.
https://doi.org/10.1007/978-3-031-76557-5_16

Polymer (FRP) composites have been evaluated in retrofitting and repairing reinforced concrete members [5]. For example, when this technique is used for RC columns' confinement, it can greatly improve bearing capacity and ductility of columns when subjected to axial loads [6, 7].

Published research [8–13] demonstrated that the hysteresis curve of columns retrofitted with unidirectional FRP is fuller than that of unconfined specimens and energy dissipation of confined specimens increased significantly. Shamim[a,b] [14, 15] conducted low-frequency full-reversal cyclic lateral loadings on RC columns combined with different axial load ratios, which indicated that the bearing capacity of columns increased with higher axial load ratios. Wang [16] retrofitted five square RC columns with CFRP (carbon fiber reinforced polymer) composites and revealed a significant improvement in energy dissipation for retrofitted concrete columns under higher axial load ratio rather than at a lower axial load ratio. Several researchers Promis [17] and Gu [18] concluded that strengthened RC columns with CFRP significantly increased bearing capacity at higher axial load ratios.

Based on the literature review conducted in this study, it is evident that column's confinement with unidirectional FRP composites increases both column's bearing capacities and ductility, however, at higher axial load levels, ductility may be affected.

In this study, columns confined with both bidirectional and multidirectional composite laminates is discussed. The experimental evaluation process involved subjecting several column specimens to low-frequency and full-reversal cyclic lateral loadings to assess seismic performance of RC columns confined with bidirectional FRP laminates considering the effect of both axial load level and the use of FRP composite anchors.

2 Description of Quasi-static Tests

2.1 Description of Column Specimens

A total of 8 reinforced concrete column specimens of 1300mm height were made, which had rectangle cross shape of 300 mm × 300 mm. The specimens were designed such that potential shear failure was avoided. The internal longitudinal steel reinforcement of each specimen comprised of four 22.0 mm-diameter steel rebars placed at the corners of cross-section, while the stirrup is in the form of 8.0 mm-diameter equally spaced at 200.0 mm. A smaller stirrup spacing of 60.0 mm was used at a distance of 300.0 mm from column top.

The axial load ratio, defined as, n, was calculated as $n = N/(f_c{}'A)$, where N represented the axial load applied at the top of the specimen, A is the column cross-sectional area, and $f_c{}'$ is the concrete axial compressive strength determined.

2.2 Design Parameters

In all tests, the values of axial load ratio, n, were taken as 0.00, 0.30, and 0.45. It should be noted that column specimens with an axial load ratio of 0.45, it approached the axial load ratio limit specified in the Code for Seismic Design of Buildings' (GB50011-2016) [19] for ordinary RC frame columns.

As mentioned earlier, three variables were tested in the experimental program included axial load ratio, bidirectional fiber laminates, and FRP anchors (See Table 1). C0, C0.3, and C0.45 represented unconfined contrast columns with axial load ratios of 0, 0.3, and 0.45, respectively. B0, B0.3, and B0.45 referred to bidirectional fiber laminates confined columns with axial load ratios of 0, 0.3, and 0.45, respectively. B0A and B0.45A correspond to bidirectional fiber laminates confined columns implemented with FRP anchors with axial load ratios of 0 and 0.45.

2.3 Material Properties

All specimens were cast by the same batch of commercial concrete, which were tested on the same day to determine the 28-day concrete compressive strength. According to China's Standard for Test Methods of Mechanical Properties of Ordinary Concrete (GB/T 50081-2016) [20], the dimensions of the cubes are 150.0 mm × 150.0 mm × 150.0 mm and the prisms are 150.0 mm × 150.0 mm × 300.0 mm. The average compressive strength of the concrete cube is 32.8 MPa, the average compressive strength of the prismatic body is 21.9 MPa, and the standard elastic modulus is 3.18 × 104 MPa.

Table 1. Column Specimens Details

Specimen ID	Axial Load Ratio	Confinement Configuration
C0	0.00	0
C0.3	0.30	0
C0.45	0.45	0
B0	0.00	2-ply bidirectional FRP laminate
B0.3	0.30	2-ply bidirectional FRP laminate
B0.45	0.45	2 layers of bidirectional FRP laminate
B0A	0	2 layers of bidirectional FRP laminate + FRP anchors
B0.45A	0.45	2 layers of bidirectional FRP laminate + FRP anchors

Notes: ***C** refers to contrast columns, **B** represents the use of bidirectional BFRP (Basalt Fiber Reinforced Polymer) full wrapping strengthening, **A** indicates the use of FRP anchors, and the numbers denote the axial load ratio*

Rebar mechanical properties were obtained by tensile coupon tests following the Chinese Standard for the Mechanical Properties of Steel (GB/T 228.1–2010) [21]. The yield strength of the longitudinal rebars and stirrups was 478.0 MPa and 358.0 MPa, respectively. The ultimate strength was 608 MPa and 470 MPa, respectively. The elastic modulus was 2.18×10^5 MPa and 2.18×10^5 MPa, respectively.

The on-axis mechanical properties of the bidirectional BFRP laminates and the two-part epoxy resin used in this study were determined experimentally (see Table 2) by the manufacturer according to the standard [22]. After conducting uniaxial tensile tests on the bidirectional laminates, the tensile strength in both orthogonal directions was almost the same.

Table 2. Mechanical Properties of BFRP Laminates and Two-Part Epoxy Resin

Composite Material	Longitudinal Compressive Strength, MPa	Longitudinal Elastic Modulus, MPa	Rupture Strain, %	Longitudinal Tensile Strength, MPa	Thickness, mm
BFRP	—	82,000	2.00	1330.00	0.33
Resin	82.6	3200	1.90	48.5	—

2.4 Loading Scheme

The test was carried out in Anhui Provincial Key Laboratory of Civil Engineering Structure and Materials, and the loading device was shown in Fig. 1. A horizontal low-cycle reciprocating load was applied using 100-ton MTS hydraulic servo actuator. The self-reaction force apparatus was used to apply high axial loads to the specimens. The specimen was placed on top of a steel base, with a rectangular groove in the middle to accommodate the reaction beam. A calibrated hydraulic jack was placed above the column, and a steel rod connected the reaction beam above the jack with the reaction beam in the steel rectangular groove. An axial load was applied using the jack, and the actual reading on the hydraulic pressure gauge was recorded once it stabilized. The base of the specimen was secured to the ground using two reaction beams and two vertical hydraulic jacks. The experiment at different axial load rations n of 0.00, 0.30, and 0.45 corresponded to actual axial loads of 0, 800.0 kN, and 1,200.0 kN, respectively.

3 Experimental Observations

All three contrast columns exhibited a flexural-shear failure mode. For column C0, during the loading process, the X-shaped diagonal tension cracks appeared on the backside of the concrete, as shown in Fig. 2a. In the case of specimen C0.3, the concrete at the column's ends crushed, and diagonal cracks appeared, as depicted in Fig. 2b. For specimen C0.45 with a higher axial load, the crack pattern at the top changed to vertical and short diagonal compression cracks, as illustrated in Fig. 2c. The increase in the axial load ratio led to a tendency for the concrete at the column's end to be more significantly crushed.

All the specimens confined with bidirectional fiber laminates (B0, B0.3, B0.45, B0A, and B0.45A) exhibited a flexural failure mode.

Near peak load of specimen B0 (refer to Fig. 3a), the final failure mode involved vertical cracks appearing on the compressed side of the column ends, and these cracks propagated diagonally upwards with each loading cycle. In the plastic hinge zone, the fiber laminates cracks widened until one side eventually delaminated. After the removal of the composite laminates, it was observed that larger concrete fragments fell and the longitudinal rebars were exposed.

In the case of B0.3, as depicted in Fig. 3b, several short transverse or diagonal cracks appeared in the plastic hinge zone in addition to the primary tearing crack as B0. After removing the FRP laminates, found that the concrete fragments were smaller compared to C0.

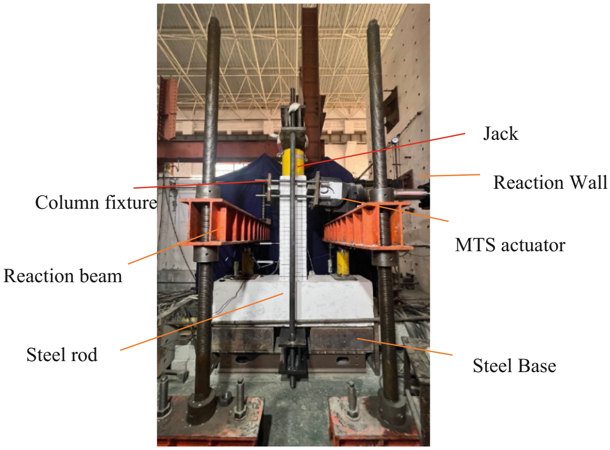

Fig. 1. Test setup

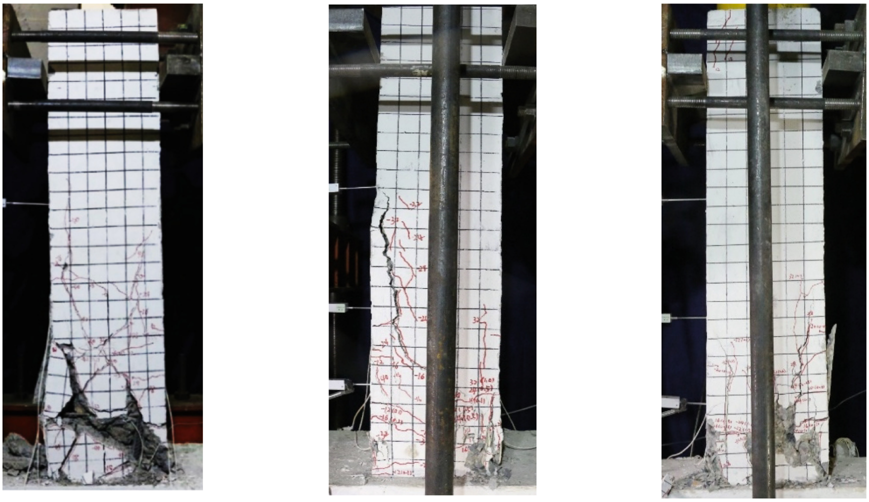

(a) C0 *(b)* C0.3 *(c)* C0.45

Fig. 2. Ultimate failure modes of unstrengthened specimens

As for specimen B0.45, the column exhibited numerous transverse short cracks in the FRP laminates, as shown in Fig. 3c. Upon removing the FRP laminates, it was evident that the concrete at the base was more thoroughly crushed.

Comparing specimens B0, B0.3, and B0.45, with the increase in the axial load ratio, the FRP laminates cracks in B0.45 gradually transitioned from diagonal primary cracks to vertical ones, and shorter transverse cracks appeared at the base. After removing the FRP laminates, it was observed that concrete expansion at the base was more pronounced, and the concrete was more thoroughly crushed.

Some obvious cracks appeared of specimen B0A near the ultimate load, and the dowel of anchor completely fractured before reaching the ultimate state. After removing FRP laminates, there were substantial diagonal cracks observed at the column base, and the concrete crushed, as seen in Fig. 3d.

In contrast, for specimen B0.45A, the dowel broke at ultimate state, and no obvious cracks were observed on FRP laminates. Only a single vertical crack was observed after removing the laminates. Additionally, fewer concrete fragments fell from the column base, as depicted in Fig. 3e.

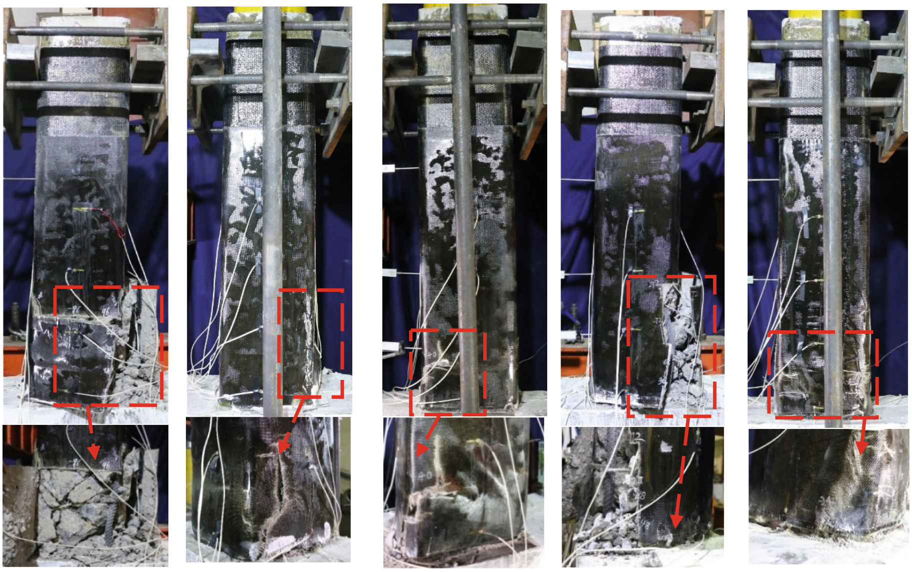

(a) B0 *(b)* B0.3 *(c)* B0.45 *(d)* B0A *(e)* B0.45A

Fig. 3. Ultimate failure mode of confined specimens

4 Experimental Results and Analysis

4.1 Hysteresis Curves

For specimens B0, B0.3, and B0.45, the hysteresis loops of the specimens' transitioned from a plump shape to a bow-shaped one as the axial load ratio increased within a certain range, which showed a pinching phenomenon (Fig. 4). The unloading stiffness of the specimens increased and the ultimate displacement reduced.

As shown in Fig. 4e and 4f, for the specimens C0.45 and B0.45, first of all, the shape of the hysteresis curve of B0.45 with confinement was fuller, and the curve pinching phenomenon was obviously improved. Secondly, the bearing capacity decreased more slowly after the peak load. Finally, the ultimate displacement of the specimen with confinement was greatly improved, which indicated that the bidirectional FRP laminates can effectively improve the deformation capacity after yielding.

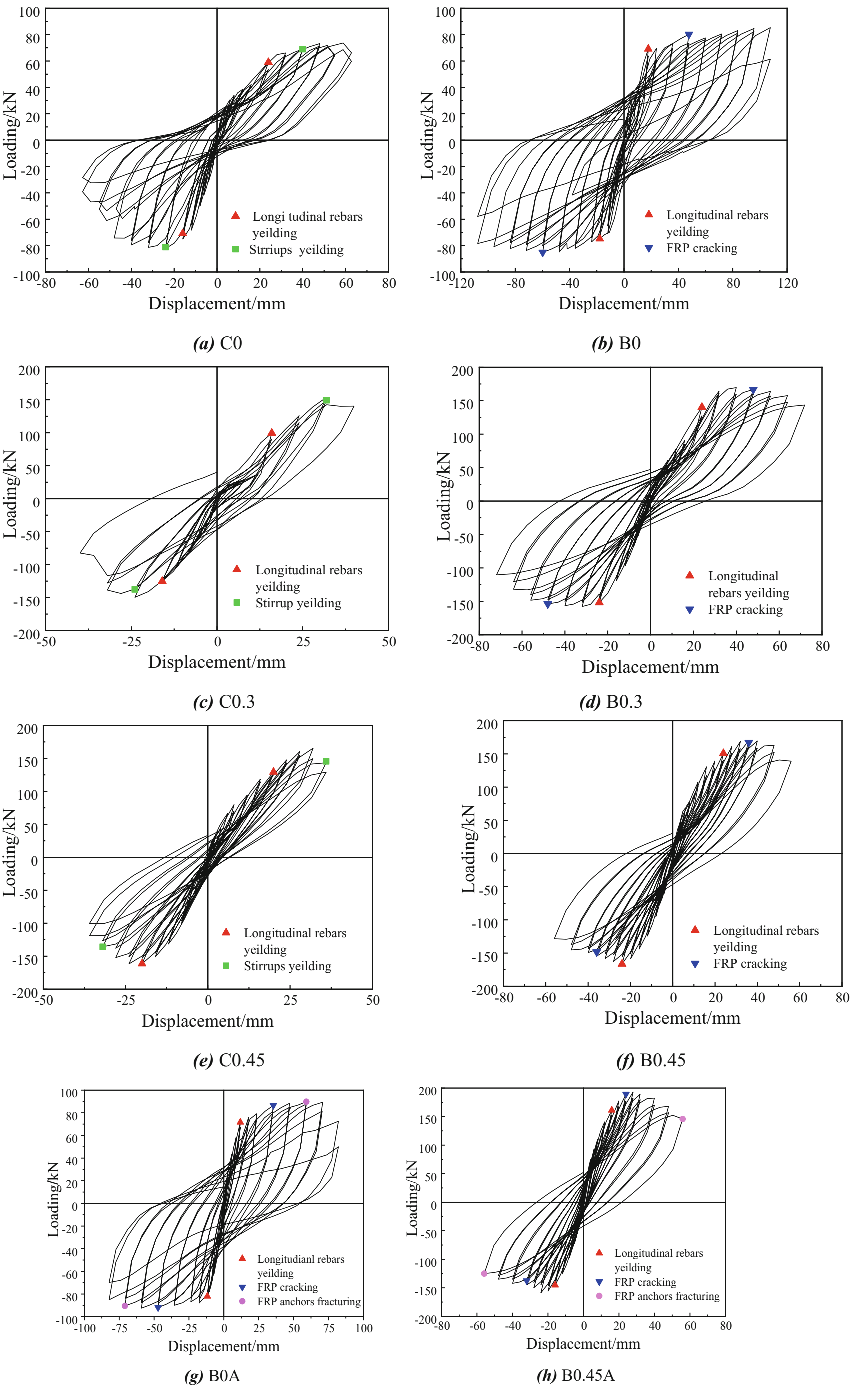

Fig. 4. Lateral load-displacement hysteretic loop curves

For specimens B0A and B0, and B0.45A and B0.45 (Fig. 4g, 4b, 4h and 4f), after installation of FRP anchors, both yield and peak load-bearing capacity of specimens B0A and B0.45A were improved. However, the displacement corresponding to FRP cracking in B0A was 30 mm, which was less than the 40 mm in B0. This is since the installation of FRP anchor increases the utilization of longitudinal fibers, which makes it easier to create stress concentration at the intersection of circumferential and longitudinal fiber, and then cracks appear in advance.

4.2 Skeleton (Envelope) Curves

As in Fig. 5, the highest point of the skeleton curve was the peak point ($\varDelta_c$, P_c). The limit point when the peak load dropped below 85% was defined as ($\varDelta_u$, P_u), and the yield point of the skeleton curve was defined as ($\varDelta_y$, P_y). The characteristics were detailed in Table 3. δP_y, δP_c and $\delta\varDelta_u$ were defined as the increase rate in yield load, peak load, and ultimate displacement of confined specimens compared to contrast specimens at the same axial load ratio.

The contrast and strengthened specimens under the same axial compression ratio were compared. As can be seen from Table 3, when the axial compression ratio was 0, 0.3 and 0.45, the δP_y of specimens B0, B0.3 and B0.45 after confinement were 26.7%, 14.1% and 10.1% compared to the contrast specimens C0, C0.3 and C0.45. Meanwhile, the δP_c values of B0, B0.3 and B0.45 were 16.3%, 13.5% and 2.7% and the $\delta\varDelta_u$ values were 68.8%, 80.0% and 55.6%. After confinement, the yield load P_y, peak load P_c and ultimate displacement $\varDelta_u$ of the specimens increased. With the increase of axial compression ratio, the yield load increase rate δP_y and peak load increase rate δP_c decrease, but the ultimate displacement increase rate $\delta\varDelta_u$ was not significantly affected.

As for specimens B0A and B0.45A, it was evident that the specimens implemented with FRP anchor exhibited the increased initial stiffness, and both yield load (P_y) and peak load (P_c) were enhanced. It can be seen that δP_y of B0A and B0.45A were 72.5% and 145.8%, and δP_c were 64.4% and 24.6%, respectively. These improvement rates were higher than those without FRP anchors B0 and B0.45.

4.3 Displacement and Ductility

The displacement ductility coefficient μ_Δ was defined as the ratio of the ultimate displacement $\varDelta_u$ to the yield displacement $\varDelta_y$, ($\mu_\Delta = \varDelta_u/\varDelta_y$). The calculation of the displacement ductility coefficient was taken as the average of the values obtained in both the positive and negative loading directions. $\delta\mu_\Delta$ was defined as the increase rate in the ductility coefficient of the confined specimens compared to the contrast specimens at the same axial load ratio.

Comparing contrast specimens with bidirectional FRP laminates confined specimens, the increase rate in the ductility coefficient $\delta\mu_\Delta$ for B0, B0.3, and B0.45 was 68.88%, 62.2, and 66.6%, respectively. The ductility coefficient increased after confinement, but the axial load ratio did not affect the increase rate of the ductility coefficient (Table. 1).

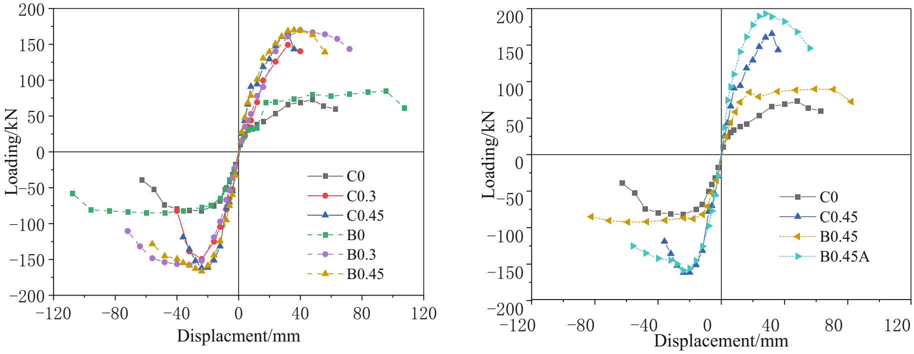

(a) C0, C0.3, C0.45, B0, B0.3 and B0.45 ***(b)*** C0,C0.45, B0.45, and B0.45A

Fig. 5. Skeleton curves of load-displacement

4.4 Energy Dissipation

Quantitative analysis of the energy dissipation capacity of the specimens was performed using cumulative energy E_{sum} and equivalent viscous damping coefficient ξ_{e}, as shown in Table 3. $\delta\xi_{\mathrm{e}}$ was defined as the increase ratio in the equivalent viscous damping coefficient of the confined specimens compared to the contrast specimens at the same axial load ratio.

Comparing the three sets of specimens B0, B0.3, and B0.45, it can be observed that the increase ratio in the equivalent viscous damping coefficient $\delta\xi_{\mathrm{e}}$ were 25.3%, 26.4%, and 46.9%, respectively. This indicated that the equivalent viscous damping coefficient increased with an increase in the axial load ratio after confinement.

Comparing B0A and B0.45A with C0 and C0.45 revealed that after the installation of FRP anchors, the $\delta\xi_{\mathrm{e}}$ for B0A and B.45A are 68.3% and 109.2%, respectively, which were higher than that for B0 and B0.45 of 23.0% and 28.3%. This implied that the installation of FRP anchors can enhance the energy dissipation capacity of the specimens, and as the axial load ratio increased, the increase ratio in energy dissipation capacity became more pronounced.

Table 3. Summary of experimental results and increase rate of the index.

Specimen	Δ_y, (mm)	P_y, (kN)	Δ_c (mm)	*Pc* (kN)	Δ_u (mm)	*Pu* (kN)	δ*Py* (%)	δ*Pc* (%)	δ*Δu* (%)	μ_Δ (mm)			$\delta\mu_\Delta$ (%)	*ESum* (kN·mm)		ξ_e		$\delta\xi_e$	
										+	-	*Avg*		*Peak*	*Ultimate*	*Peak*	*Ultimate*	*Peak*	*Ultimate*
C0	18.0	47.5	48.0	73.2	64.0	59.7	–	–	–	60	4.6	4.1	–	9,517	16,695	0.126	0.188	–	–
C0.3	23.3	125.5	32.0	149.3	40.0	140.4	–	–	–	40	2.2	2	–	6,951	12,345	0.104	0.154	–	–
C0.45	21.5	137.2	32.0	165.5	36.0	143.3	–	–	–	34	1.9	1.8	–	3,882	8,726	0.078	0.115	–	–
B0	16.3	60.2	60.0	85.1	108.0	61.4	26.7	16.3	68.8	108	7	6.4	66.6	17,242	53,087	0.155	0.236	23.0%	25.3%
B0.3	24.1	143.2	40.0	169.5	72.0	143.5	14.1	13.5	80.0	72	3.4	3.2	62.2	14,563	42,291	0.133	0.195	27.2%	26.4%
B0.45	22.6	151.1	36.0	170.0	56.0	131.5	10.1	2.7	66.6	52	3.2	3	66.6	9,067	19,256	0.100	0.172	28.3%	49.6%
B0A	12.5	78.1	60.0	92.5	84.0	72.5	64.4	26.4	31.3	84	7.6	7.3	77.4	20,746	37,594	0.212	0.201	68.3%	6.8%
B0.45A	18.9	165.5	28.0	193.1	56.0	145.8	20.6	16.7	55.6	56	3.2	3.1	71.1	11,883	23,034	0.163	0.193	109.2%	68.1%

Note: *δ_{Py}, δ_{Pc}, $\delta_{\Delta u}$, $\delta_{\mu\Delta}$ and $\delta\xi_e$ are the increase rate of yield load, peak load, ultimate displacement, displacement ductility coefficient and equivalent viscous damping coefficient of the specimen under confinement compared with contrast members. For example, the yield load increase rate δP_y of the bidirectional fiber laminate specimen B0.3 is the difference between P_y of B0.3 and P_y of C0.3 divided by P_y of C0.3*

5 Conclusions

The study focused on investigating the influence of axial load ratios and FRP anchors on the seismic performance of RC columns with bidirectional FRP laminates. Eight specimens were divided into three groups and subjected to low-cycle cyclic loading tests. Through analysis of the test results and theoretical research, the following conclusions were as follows:

The failure modes of bidirectional FRP laminates differed significantly from traditional unidirectional fiber sheets. The confined specimens changed from flexural-shear failure to flexural failure. The hysteresis curves became more plump, pinching effects were improved and energy dissipation and deformation capacity were enhanced.

As the axial load ratio increased for confined specimens B0, B0.3 and B0.45, the increase rate of bearing capacity decreased with higher axial load ratios. The increase rate in yield load capacity was more noticeable than the peak load capacity. The yield load capacity increased by 16.3%, 13.5%, and 2.7%, and the peak load capacity increased by 26.7%, 14.1%, and 10.1%. The axial load ratio had a less pronounced effect on the increase in displacement ductility, but energy dissipation capacity increased with higher axial load ratios. The displacement ductility coefficient increased by 66.6%, 62.2%, and 66.6%, and energy dissipation capacity increased by 25.3%, 26.4%, and 49.6% with increasing axial load ratios after confinement for B0, B0.3 and B0.45.

The installation of anchor bolts enhanced the energy dissipation capacity of the specimens, and the increase rate of energy dissipation capacity became more significant with higher axial load ratios. After the installation of anchors, the $\delta\ \xi_{\mathrm{e}}$ for B0A and B.45A were 68.3% and 109.2%, respectively, which were higher than the values for B0 and B0.45 at 23.0% and 28.3%.

References

1. Qin, Z., Na, W., Jinxin, G.: State of the art of seismic performance including shear effects and failure modes of reinforced concrete columns. J. Build. Struct. **38**(8), 1–13 (2017)
2. Hosseinpour, F., Abdelnaby, A.E.: Effect of different aspects of multiple earthquakes on the nonlinear behavior of RC structures. Soil Dyn. Earthq. Eng. **92**(2), 702–725 (2017)
3. Jian, Y., Sla, B., Xz, C., et al.: Experimental research and finite element analysis on the seismic behavior of CFRP-strengthened severely seismic-damaged RC columns. Structures **34**, 3968–3981 (2021)
4. Cui, Z., Alice, A., Behrouz, S.: Structural performance of fiber-reinforced concrete columns. Mater. Struct. **191**, 460–468 (2019)
5. Mosallam, A.S., Bayraktar A, Elmikawi M, Pul S, Adanur S. Polymer composites in construction: an overview. SOJ Mat. Sci. Eng. (2014). https://symbiosisonlinepublishing.com/materialsscience-engineering/materialsscience-engineering07.php
6. Haroun, M.A., Mosallam, A.S., Feng, M.Q., Elsanadedy, H.M.: Experimental investigation of seismic repair and retrofit of bridge columns by composite jackets. J. Reinf. Plast. Compos. **22**(14), 1243–1268 (2003)
7. Youssef, M.N., Feng, M.Q., Mosallam, A.S.: Stress–strain model for concrete confined by FRP composites. Compos. B Eng. **38**(5–6), 614–628 (2007)
8. Ouyang, L.J., Gao, W.Y., Zhen, B., Lu, Z.D.: Seismic retrofit of square reinforced concrete columns using basalt and carbon fiber-reinforced polymer sheets: a comparative study. Compos. Struct. **162**, 294–307 (2017)

9. Promis, G., Ferrier, E.: Performance indices to assess the efficiency of external FRP retrofitting of reinforced concrete short columns for seismic strengthening. Constr. Build. Mater. **26**, 32–40 (2012)
10. Jun, J., Zenga, B., Yongchang, G., et al.: Stress-strain behavior of concrete in circular concrete columns partially wrapped with FRP strips. Compos. Struct. **200**, 810–828 (2018)
11. Wang, D., Huang, L., Yu, T., Wang, Z.: Seismic performance of CFRP-retrofitted large-scale square RC columns with high axial compression ratios. J. Compos. Constr. **21**(5), 04017031 (2017)
12. Paultre, P., Boucher-Trudeau, M.: Behavior of circular reinforced-concrete columns confined with carbon fiber-reinforced polymers under cyclic flexure and constant axial load. Compos. Struct. **20**(3), 04015065 (2016)
13. Gu, D.S., Wu, Y.F., Wu, G., Wu, Z.S.: Plastic hinge analysis of FRP confined circular concrete columns. Constr. Build. Mater. **27**(1), 223–233 (2012)
14. [a] Shamim, A.S., Yau, G.: Seismic behavior of concrete columns confined with steel and fiber-reinforced polymers. ACI Struct. J. **99**(01), 71–80 (2002)
15. Shamim, A.S.: Performance of concrete structures retrofitted with fiber-reinforced polymers. Eng. Struct. **24**, 869–879 (2002)
16. Daiyu, W., Le, H., Tao, Y.: Seismic performance of CFRP-retrofitted large-scale square RC columns with high axial compression ratios. Compos. Struct. **21**(5), 04017031 (2017)
17. Promis, G., Ferrier, E.: Performance indices to assess the efficiency of external FRP retrofitting of reinforced concrete short columns for seismic strengthening. Constr. Build. Mater. **26**(3), 32–40 (2012)
18. Dongsheng, G., Gang, W., Zhishen, W.: Confinement effectiveness of FRP in retrofitting circular concrete columns under simulated seismic load. Compos. Struct. **14**(5), 531–540 (2010)
19. Ministry of Construction of the People's Republic of China. GB 50011–2016, Code of seismic design of buildings. China Architecture and Building Press, Beijing (2016). (in Chinese)
20. Ministry of Construction of the People's Republic of China. GB/T 50081–2016, Standard for test method of mechanical properties on ordinary concrete. China Architecture and Building Press, Beijing (2016). (in Chinese)
21. General Administration of Quality Supervision, Inspection and Quarantine of the People's Republic of China. GB/T 228.1–2010, Metallic Materials-Tensile testing-Part 1: Method of test at room temperature. Standards Press of China, Beijing (2010). (in Chinese)
22. Ministry of Housing and Urban-Rural Development of the People's Republic of China. GB 50728-2011, Technical code for safety appraisal of engineering structural strengthening materials. China Architecture and Building Press, Beijing (2011). (in Chinese)